Controlled Modulation of the Helical Sense and the Elongation of Poly(phenylacetylene)s by Polar and Donor Effects

Seila Leiras, Félix Freire*, José Manuel Seco, Emilio Quiñoá, Ricardo Riguera*

Center for Research in Biological Chemistry and Molecular Materials (CIQUS)
and Department of Organic Chemistry, University of Santiago de Compostela,
E-15782 Santiago de Compostela, Spain

ricardo.riguera@usc.es, felix.freire@usc.es

http://www.usc.es/gi1608/

Electronic Supplementary Information

Contents:

Synthesis of monomers (*R*)- and (*S*)-1

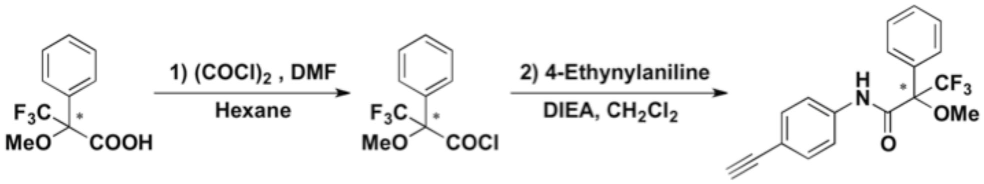

Oxalyl chloride (2.5 mL, 1.4 equiv) was added dropwise to a solution of *(R)*- or *(S)*-α-methoxy-α-(trifluoromethyl)phenylacetic acid (1.00 g, 1.0 equiv) in dry hexane and DMF (300 μL, 1.0 equiv) at 0 ºC under an Ar atm. After 4 h stirring at rt, the reaction mixture was filtered and the solution obtained dried under vacuum to give the acetyl chloride as colorless oil in quantitative yield.

The *(S)*- or *(R)*-α-methoxy-α-(trifluoromethyl)phenylacetyl chloride obtained, (1.07 g, 1.0 equiv) was dissolved in CH_2Cl_2 (40.0 mL) and diisopropyltriethylamine (DIEA, 1.2 mL, 1.6 equiv) and 4-ethynilaniline (500.0 mg, 1.0 equiv) where added to the solution. The reaction mixture was stirred at rt overnight. The residue was diluted with CH_2Cl_2 and the organic solution was washed with HCl 1M, saturated $Na(HCO_3)$ aq solution and saturated NaCl aq solution; then the organic layer was dried over anhyd Na_2SO_4. After filtration, the solution was evaporated and the residue was chromatographed on silica gel with hexane-AcOEt (7/3, v/v) as the eluent [1.30 g (*R*)-1 and 1.28 g *(S)*-2], 91% and 90 % yield respectively of pure products).

Spectroscopic Data (Figure S1):

(*R*)-N-(4-ethynylphenyl)-3,3,3-trifluoro-2-methoxy-2-phenylpropanamide (2):

α_D = +68.2 (c = 10.0 mg/mL, $CHCl_3$). Mp = 87 ºC

^{1}H NMR (300 MHz, $CHCl_3$) δ(ppm): 3.04 (s, 1H), 3.47 (s, 3H), 7.40-7.50 (m, 5H), 7.52-7.57 (m, 4H), 8.61 (broad s, 1H)

^{19}F NMR (282.3 MHz, $CHCl_3$) δ(ppm): - 68.7

^{13}C NMR (100 MHz, $CHCl_3$) δ(ppm): 55.2, 83.1, 118.5, 119.5, 127.7, 128.0, 128.8, 129.0, 129.8, 132.0, 133.0, 137.1, 164.3.

HRMS (ESI) m/z calcd for $C_{18}H_{15}F_3NO_2$ [M+H]: 334.1010, found: 334.1039.

(*S*)-N-(4-ethynylphenyl)-3,3,3-trifluoro-2-methoxy-2 phenylpropanamide:

α_D = -67.7 (c = 10.0 mg/mL, $CHCl_3$). Mp= 88 ºC

^{1}H NMR (300 MHz, $CHCl_3$) δ(ppm): 3.04 (s, 1H), 3.47 (s, 3H), 7.40-7.50 (m, 5H), 7.52-7.57 (m, 4H), 8.61 (broad s, 1H).

^{19}F NMR (282.3 MHz, $CHCl_3$) δ(ppm): -68.7.

^{13}C NMR (100 MHz, $CHCl_3$) δ(ppm): 55.2, 83.1, 118.5, 119.5, 127.7, 128.0, 128.8, 129.0, 129.8, 132.0, 133.0, 137.1, 164.3.

HRMS (ESI) m/z calcd for $C_{18}H_{15}F_3NO_2$ [M + H]: 334.1010, found: 334.1049.

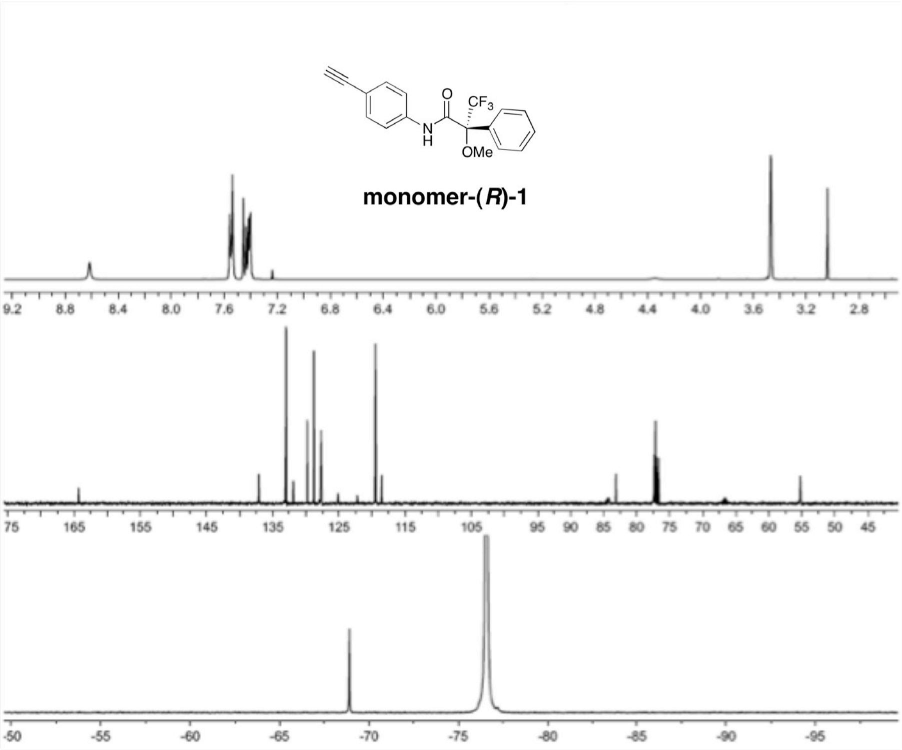

Figure S1: ^{1}H, ^{13}C NMR and ^{19}F spectra of monomer (*R*)-**1** ($CDCl_3$, 300 MHz).

Conformational studies of monomers (*R*)- and (*S*)-1

Theoretical calculations

To investigate the conformational composition of monomers (*R*)- and (*S*)-**1**, DFT calculations (B3LYP-6-31G*) were performed. These computational studies were done by using the Gaussian09 software package. During these studies we checked all the possible conformations for the (O=)C-N(-H) and the (O=)C-C(-O) bonds, finding that the lowest energy conformers present the amide bond in trans configuration and the (O=)C-C(-O) in *ap* conformation (carbonyl and methoxy group in antiperiplanar orientation). We denoted this conformer as *trans-ap*. The second conformer in lowest energy is *trans-sp* (amide in trans and the (O=)C-C(-O) in synperiplanar orientation), being 4.5 Kcal/mol less stable than the trans-ap. Finally, the cis-ap conformer (amide in cis configuration and the (O=)C-C(-O) bond antiperiplanar oriented) is the highest energy conformer, being 8.8 Kcal/mol less stable than the *trans-ap*. Similar results were obtained when the studies were carried out taking into account the dielectric constant of the solvent. (see Figure S2)

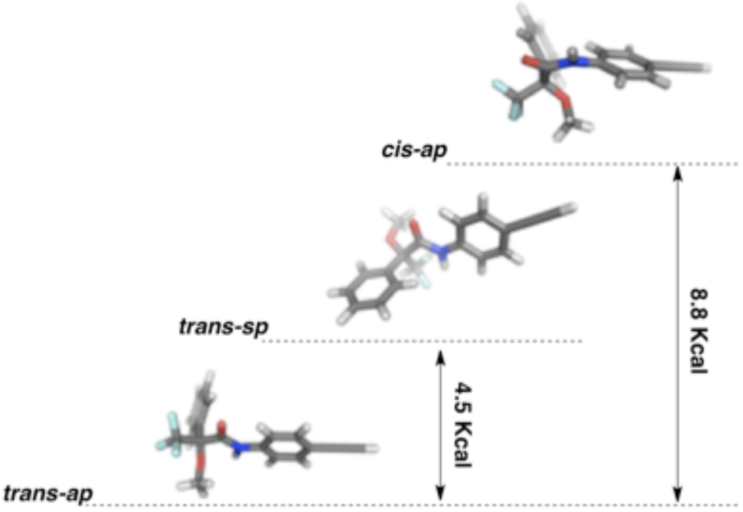

Figure S2: Major conformers of monomer (*R*)-**1** obtained with DFT calculations.

CD Studies

The “Octant Rule” approach was applied to study the conformation of the (O=)C-C(-O) bond by CD. Thus, if the major conformer in the *(R)*-MTPA derivative is *ap* (C=O and OMe antiperiplanar oriented), we should observe a positive Cotton effect in the CD spectrum, whereas if the major conformer is *sp* (synperiplanar), the Cotton effect should be negative (Table S1)

The CD spectra of monomer (*R*)- and (*S*)-**1** were recorded in different solvents. The results obtained reveal a positive Cotton effect for monomer (*R*)-**1** in all the solvents used, whereas the opposite sign was observed for monomer (*S*)-**1**. This indicates that ap is the preferred conformation for the (O=)C-C(-O) bond in all the cases (Figure S5).

	(*R*)-MTPA		**(*S*)-MTPA**	
Conformer	***sp***	***ap***	***sp***	***ap***
Cotton effect	**Negative**	**Positive**	**Positive**	**Negative**
	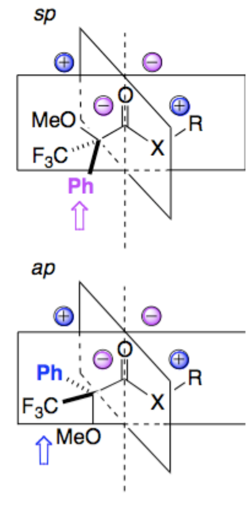		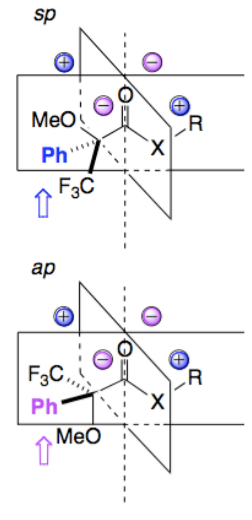	

Table S1: Expected Cotton effects signs of *sp* and *ap* MTPA conformers by applying the Octant Rule.

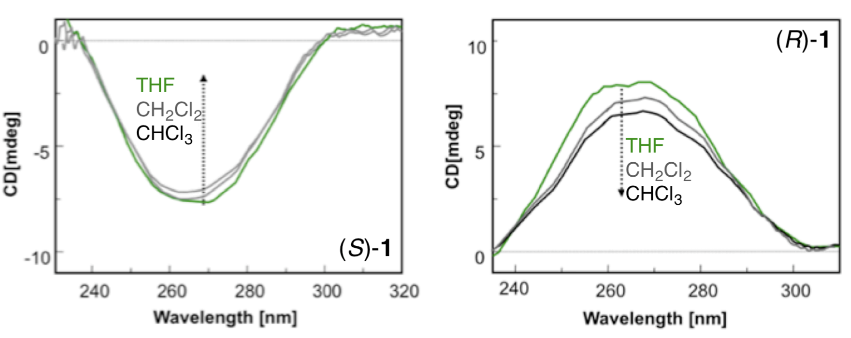

Figure S3: CD spectra of monomer (*R*)-**1** and monomer (*S*)-**1** (0.5 mM concn).

UV-Vis Studies

UV-Vis spectra of the monomers show variations in absorbance intensity due to small conformational changes associated to the type of solvent used.

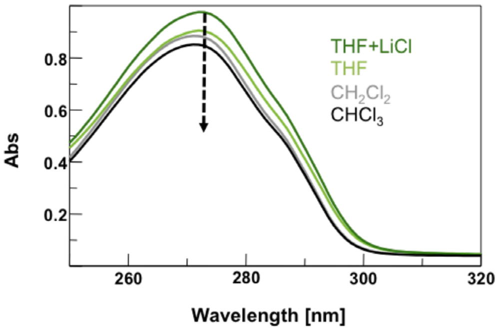

Figure S4: UV-Vis spectra of monomer (*R*)**-1** in several solvents. Similar spectra were observed for monomer (*S*)**-1** (0.5 mM concn).

Optical Rotation Studies

The values obtained for the optical rotation measurements, despite having the same sign, were different depending on solvent used. This fact may indicate a small change in populations among the possible conformers (i.e. *cis-sp*, *cis-ap*, and *trans-ap*). These differences became more noticeable for THF and acetone, both donor solvents. The concentration of monomer in all the samples was 0.01 g/mL.

	$CHCl_3$	CH_2Cl_2	THF	Acetone
(*S*)-**1**	-67.70	-75.27	-196.45	-133.18
(*R*)-**1**	+68.15	+75.41	+186.10	+143.00

Table S2: Optical Rotation values for monomer (*R*)- and (*S*)-***1*** in different solvents.

NMR Studies

NMR experiments were carried out in order to have more precise information about the conformation of the monomers.

Heteronuclear $^{19}F–^{1}H$ HOESY was performed in different solvents. A NOE effect was observed in all the experiments among the fluorine atoms and both the OMe protons and the aromatic protons (Figure S5). However, NOE was not observed between the N-H proton and the CF_3. This fact is indicative of the presence of the *ap* conformation for the (O=)C-C(-O) bond.

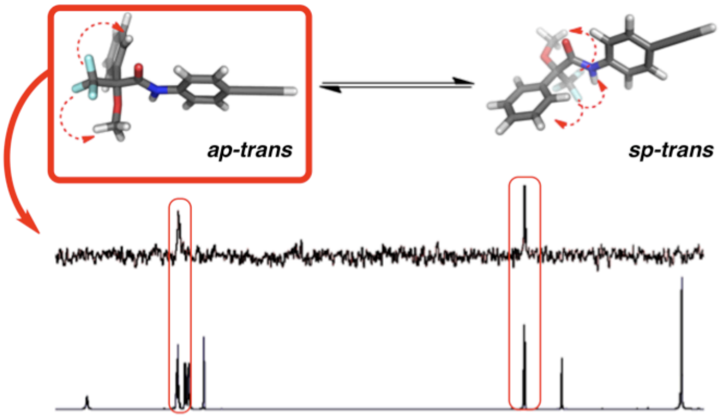

Figure S5: HOESY $^{19}F–^{1}H$ spectra of monomer (*R*)-***1*** in $CDCl_3$.

X-Ray Studies

Different samples where prepared in order to perform X-Ray measurements. The crystals where prepared in a mixture of hexane and the solvents of interest, $CHCl_3$, CH_2Cl_2, THF and acetone, where the same lattice was found for all of them: amide in *trans* and the (O=)C-C(-O) bond in *ap* conformation (Figure S6).

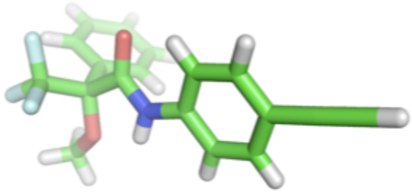

Figure S6: X-Ray structure for monomer (*R*)-***1***.

Synthesis of polymers poly-(*R*)- and (*S*)-1.

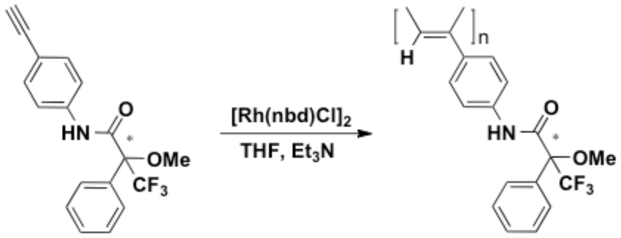

The reaction flask (sealed ampoule) was dried under vacuum and Ar flushed for three times before monomer (*R*)-***1*** (200.0 mg, 0.5 M) was added as a solid. Then, the flask was evacuated on a vacuum line and flushed with dry Ar (three times). Dry THF (1000 µL) and Et_3N (10 µL, 0.05 M) were added via a syringe. A solution of rhodium norbornadiene chloride dimmer (2.7 mg), $[Rh(nbd)Cl]_2$, in THF (200 µL) was added at 30 ºC. The reaction mixture was stirred at 30 ºC for 2 h. Then, the resulting polymer (poly-**1**) was diluted in THF and precipitated in a large amount of MeOH, centrifuged (2 times) and reprecipitated in hexane and centrifuged again (178.2 mg, 89% yield). Analogous procedure was employed to prepare poly-(*S*)-***1***.

Spectroscopic Data (Figures S7 and S8)

The *cis* stereoregularity of poly-(*R*)-***1*** was determined by ^{1}H NMR spectroscopy[I], where the vinyl proton resonates at 5.8 ppm (Figure S7), and Raman Resonances[II] (Figure S8). The peak at 1567 cm^{-1} is assigned to C=C bond stretching in the *cis* polyacetylene and overlaps with that of the phenyl ring. The peak at 1336 cm^{-1} is assigned to the *cis* C-C bond coupled with the single bond connecting the main chain and the phenyl ring. The peak at 1003 cm^{-1} is assigned to the C-H bond deformation of the cis form. Identical NMR and Ramman spectra were obtained for the enantiomeric polymer, poly-(*S*)-**1**.

Raman spectra were performed in a confocal Renishaw Raman spectrometer (Invia Reflex model) equipped by 785 nm diode laser, Ion Ar 514 nm. (350 mW, 1.064 nm excitation wavelength). NMR experiments were carried out in a Varian Inova 750 spectrometer, 17.61 T magnetic field.

Poly-(*R*)-*1*:

α_D = -379.3 (c = 7.5 mg/mL, $CHCl_3$).

^{1}H NMR (750 MHz, $CDCl_3$) δ(ppm): 3.41 (s, br, 3H), 5.78 (s, br, 1H), 6.47 (s, broad, 2H), 7.20 – 7.50 (d, br, 7H), 8.59 (broad , 1H).

^{19}F NMR (282.3 MHz, $CDCl_3$) δ(ppm): - 68.0.

^{13}C NMR (100 MHz, CDCl$_3$) δ(ppm): 54.9, 89.3, 119.6, 123.0, 125.2, 127.8, 128.6, 132.2, 135.4, 138.4, 162.9.

Molecular weight (Mn): 102000; Mw/Mp = 2.2. [THF as eluent at a flow rate of 1 mL/min and a concentration of 2 g/L using narrow polystyrene standards (PSS) as calibrants].

Poly-(*S*)-*1*:

α_D = +353.1 (c = 7.5 mg/mL, CHCl$_3$).

^{1}H NMR (750 MHz, CDCl$_3$) δ(ppm): 3.41 (s, br, 3H), 5.78 (s, br, 1H), 6.47 (s, broad, 2H), 7.20 – 7.50 (d, br, 7H), 8.59 (broad s, 1H).

^{19}F NMR (282.3 MHz, CDCl$_3$) δ(ppm): - 68.0.

^{13}C NMR (100 MHz, CDCl$_3$) δ(ppm): 54.9, 89.3, 119.6, 123.0, 125.2, 127.8, 128.6, 132.2, 135.4, 138.4, 162.9.

Molecular weight (Mn): 60100; Mw/Mp = 1.4. (THF as eluent at a flow rate of 1 mL/min and a concentration of 2 g/L using narrow polystyrene standards (PSS) as calibrants).

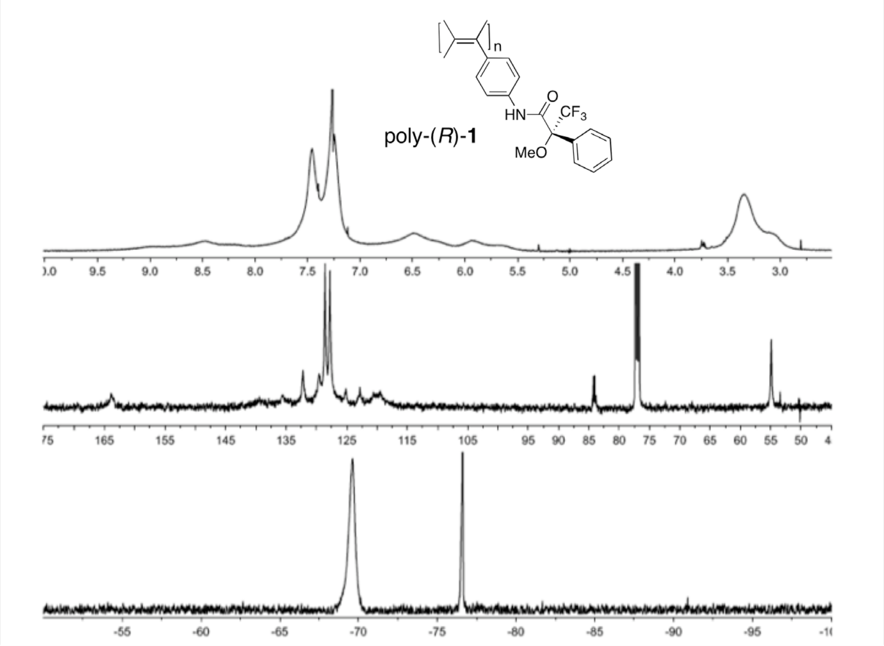

Figure S7: ^{1}H, ^{13}C and ^{19}F spectra of poly-(*R*)-**1**.

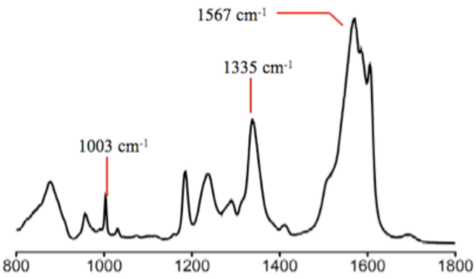

Figure S8: Raman spectrum for poly-(*R*)-**1**.

Structural Studies on poly-(*R*)-1

CD in different solvents

Solutions of poly-(*R*)-**1** were prepared combining different solvents (0.5 mM). The CD spectra of the polymer change in sign and magnitude depending not only on the polarity of the solvent, as reported previously for other PPAs[III] , but also depending on its donor properties.

	$CHCl_3$	THF	CH_2Cl_2	1,2-CH_4Cl_2	Acetone	DMF
(ε-1)/(ε+1)	0.656	0.767	0.799	0.824	0.908	0.947
CD [mdeg]	-14.34	22.7	-3.7	-2.57	-3.9	-10.72

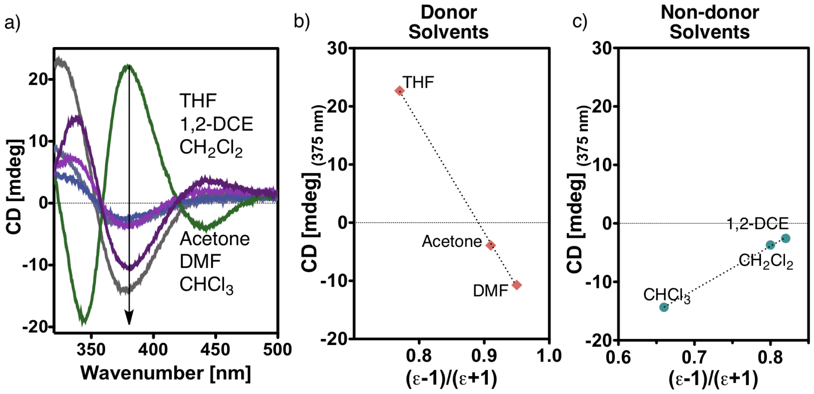

Figure S9: a) CD spectra of poly-(*R*)-**1** in different solvents. b) Representation of CD intensities vs. polarity parameters.

	$CHCl_3$	THF	Acetone	CH_3CN	DMSO
(ε-1)/(ε+1)	0.656	0.767	0.908	0.948	0.958
CD [mdeg]	-11.25	-2.57	3.21	3.28	3.39

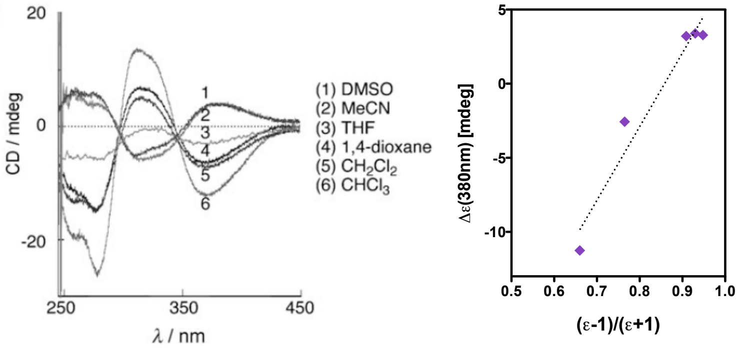

Figure S10: For comparison purposes, an example of direct dependence of the helical conformation with the solvent polarity is depicted here, corresponding to the CD spectra and the representation of CD intensities vs. polarity parameters of poly-phenylglycine-OMe in different solvents.

UV-Vis in different solvents

In order to obtain further information about conformational changes in poly-(*R*)-**1**, UV-Vis spectra where registered in different solvents. For these experiments, we prepared solutions using a concentration of 0.5 mM.

The results obtained were consistent with those obtained for CD studies. It is possible to see differences both in absorbance intensity and bathochromic displacements at the vinylic region associated to the polar effect and the donor capacity of the solvents.

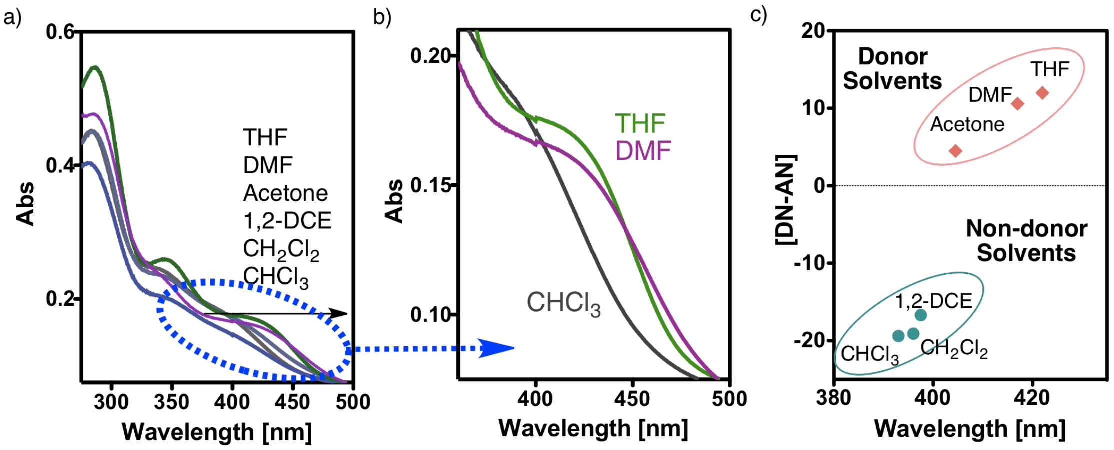

Figure S11: a) and b) UV-Vis spectra of poly-(*R*)-**1** in different solvents. c) Representation of UV-Vis wavelength absorption vs. [DN-AN] Gutmann values.

Accordingly to the mentioned parameters and the experimental data obtained, we can arrange solvents into four groups according to the 4 different helical conformations they generate: (left-handed compressed, left-handed extended, right-handed compressed and right-handed extended): 1) non-donor/low-polar, 2) donor/low-polar, 3) non-donor/polar and 4) and donor/polar solvents.

Studies of the effect of donor solvents on the conformation of poly-(*R*)-1 by CD and UV-Vis

Donor solvents, described as having a high acceptor number (AN) and low donor number (DN), can be classified into two main groups according to their polarity properties and that correspond to different families of functional groups. Hence, we can classify ethers and amines in the first group (donor and low-polar solvents) and ketones, esters, amides and sulfoxides in the second group.

1. *Ethers and amines*: These low-polar solvents with high donor capacity and low acceptor properties make poly-(*R*)-**1** to adopt the preferred *cis*-*ap* conformation (Scheme S1). Titration studies were preformed in order to demonstrate this conception. In most of the titrations done, the addition of high amounts of solvent was not possible due to solubility problems. Therefore, in order to study the helicity, 1.85 mM of several ethers and amines were added to a 0.5 mM solution of poly-(*R*)-**1**. The results obtained show how solvents such as THF, dioxane or isopropylamine induce the helix inversion as well as the chain elongation, easily observed both in the CD signature and in the UV-Vis spectra and shown in the next section. It is also important to mention that steric hindrance plays an important role in the helical conformation since more voluminous solvents, such as buthylether or triethylamine, either reveal difficulties to invert the helicity or do not invert the helical conformation (see Figures S12-14).

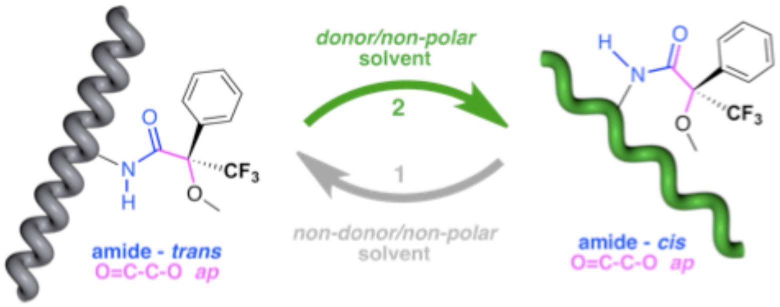

Scheme S1: Conformational equilibrium for poly-(*R*)-**1** low-polar solvents.

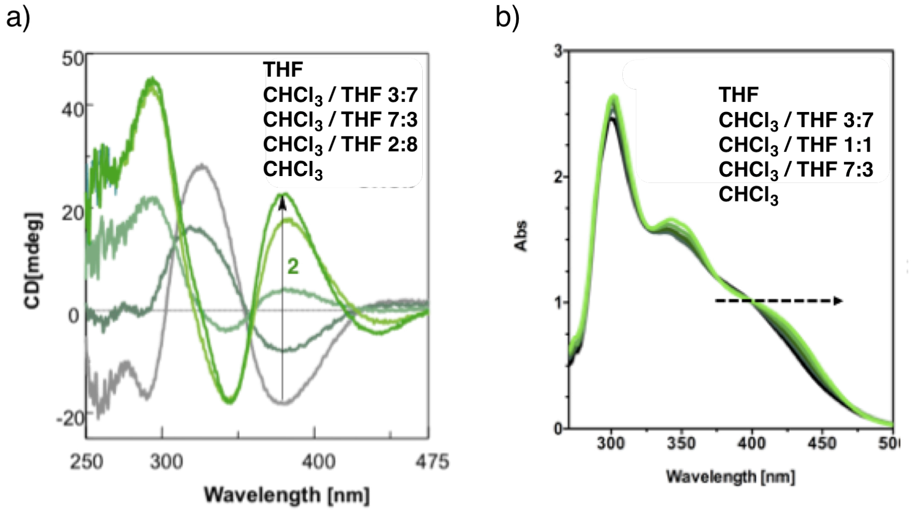

Figure S12: a) CD spectra and b) UV-Vis spectra of the titration for poly-(*R*)-**1** in THF/CHCl$_3$, where it is possible to observe progressive changes due to helical inversion (a) and chain elongation (b).

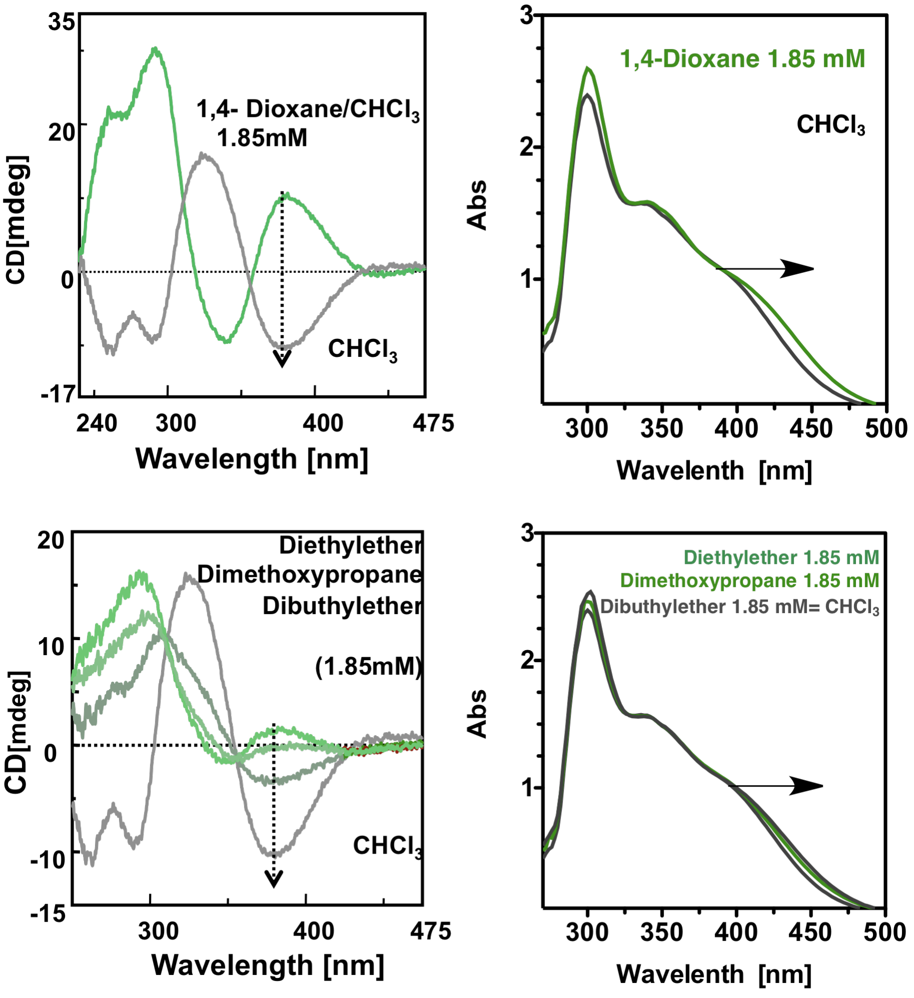

Figure S13: CD and UV-Vis spectra of poly-(*R*)-**1** in different ethers.

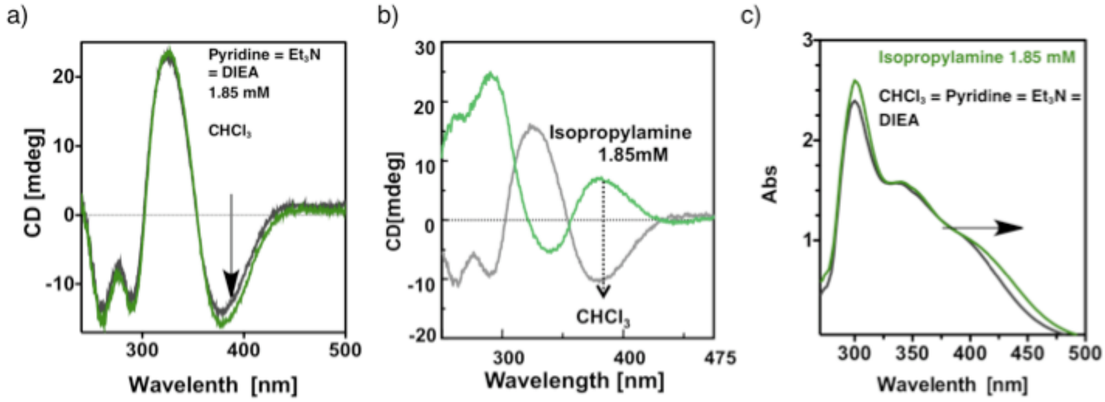

Figure S14: CD and UV-Vis spectra of poly-(*R*)-**1** in different amines.

2. *Ketones, amides, esters and sulfoxides:* These families of functional groups are polar compounds that have high donor capacity and medium acceptor properties that favor the equilibrium represented in Scheme S2. In order to study their effects in the polymer conformation, several titrations combining different proportions of $CHCl_3$ and the solvent of interest were done. Thus, in this case a major difference was observed with respect of the results obtained for low-polar/non-donor solvents. We can observe a "double inversion" on the polymer conformation: when little amount of solvent is added to the $CHCl_3$ solution (up to 40% of total amount, approximately) the helical conformation is inverted. If further solvent proportion is added, the helical conformation is inverted again and elongated. See the main body of the manuscript for discussion of the mechanism. In accordance with the proposed mechanisms, hindered solvents such as 4-phenyl-butan-2-one just carry out the first effect, (modification of the *ap*-*sp* equilibrium; see Figures S15-17).

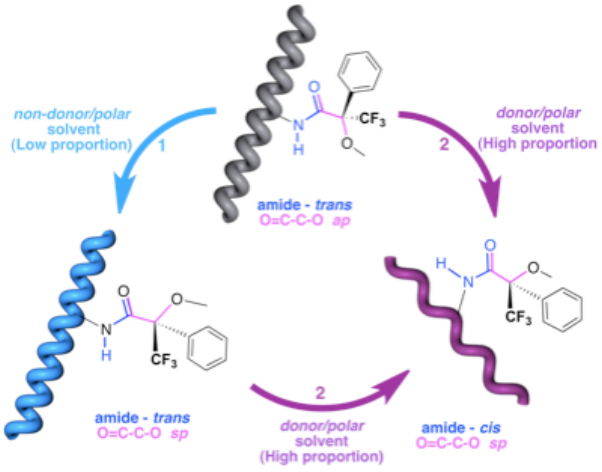

Scheme S2: Conformational equilibrium of poly-(*R*)-**1** in polar/donor solvents (ketones, amides, sulfoxides).

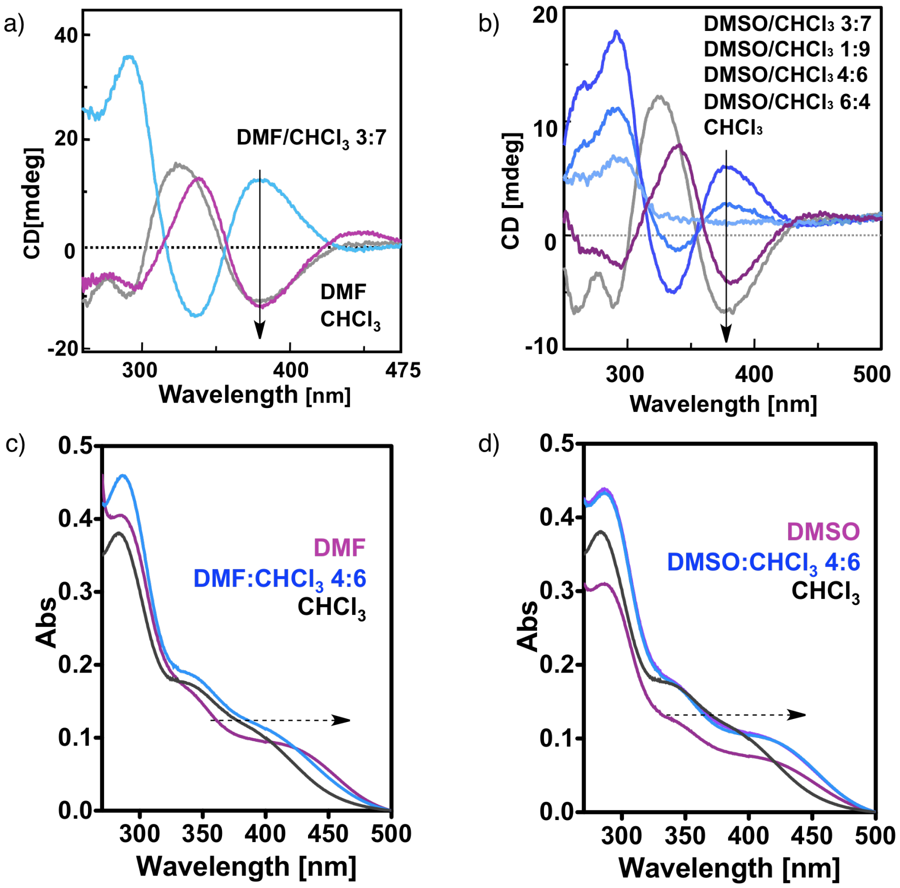

Figure S15: CD, a) and b), and UV-Vis spectra, c) and d), of poly-(*R*)-**1** in DMF and DMSO, respectively.

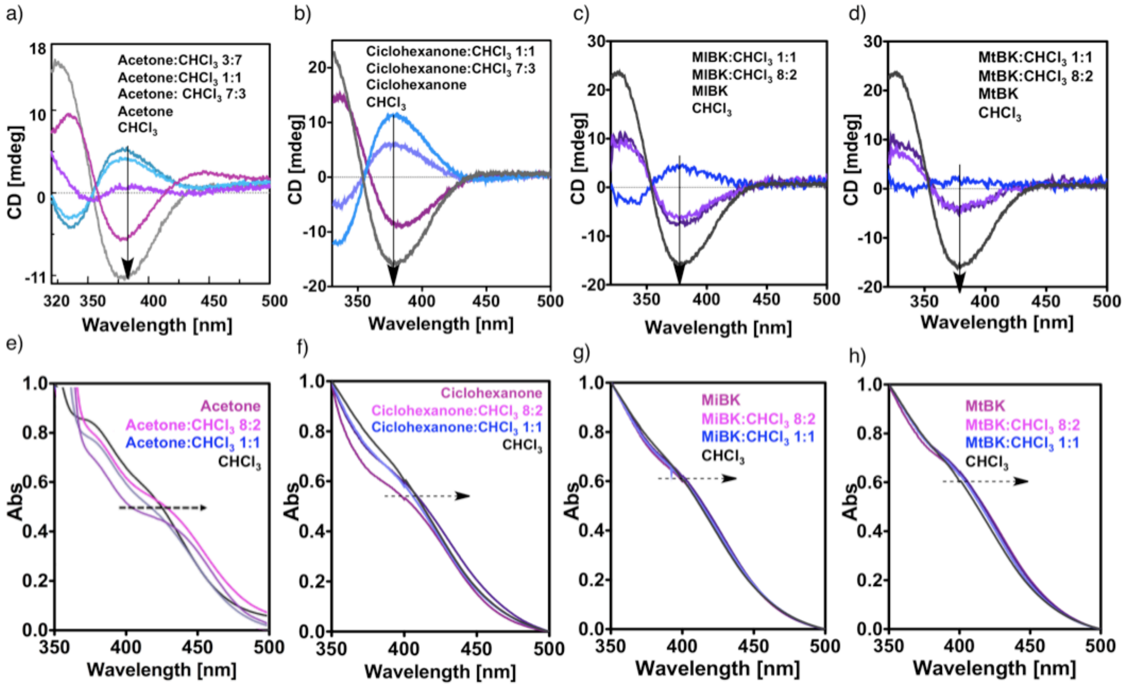

Figure S16: a), b), c) and d) CD and e), f), g) and h) UV-Vis spectra of poly-(*R*)-**1** in different ketones.

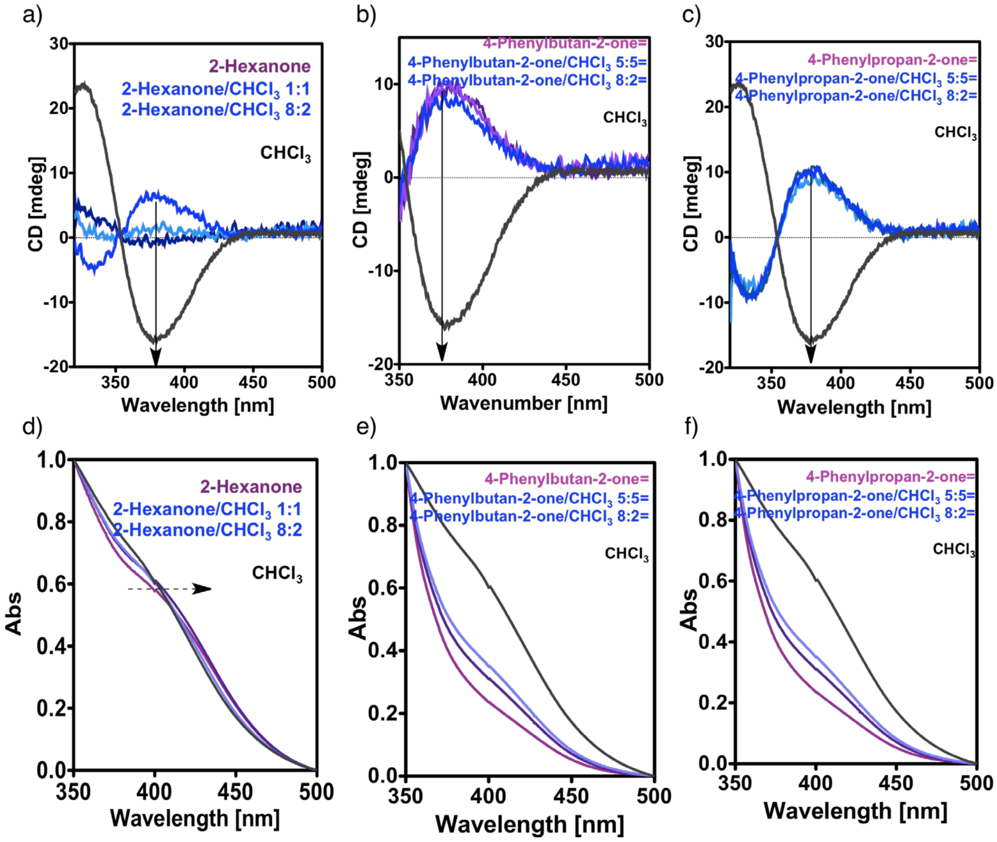

Figure S17: a), b) and c) CD and d), e) and f) UV-Vis spectra of poly-(*R*)-**1** in different hindered ketones.

Studies of the effect of non-donor solvents on the conformation of poly-(*R*)-1 by CD and UV-Vis

Non-donor solvents, with high acceptor (AN) and low donor (DN) numbers, are described as having low coordinating capacity. We can classify into this group solvents such as haloalkanes, that have a relative low-polarity (i.e $CHCl_3$), or alcohols with higher polarity properties (i.e. MeOH). Their effect in the polymer conformation it is based on the manipulation of the *ap*-*sp* equilibrium depending on the polarity of the solvent used; i.e the addition of non-donor and polar solvents favors the *ap*-*sp* equilibrium towards the sp conformation, see Scheme S3.

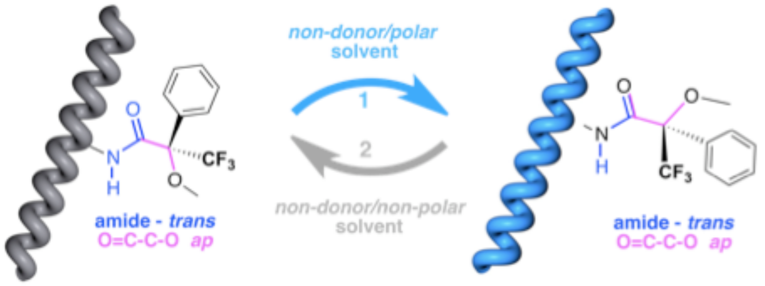

Scheme S3: Conformational equilibrium for polar and non-donor solvents

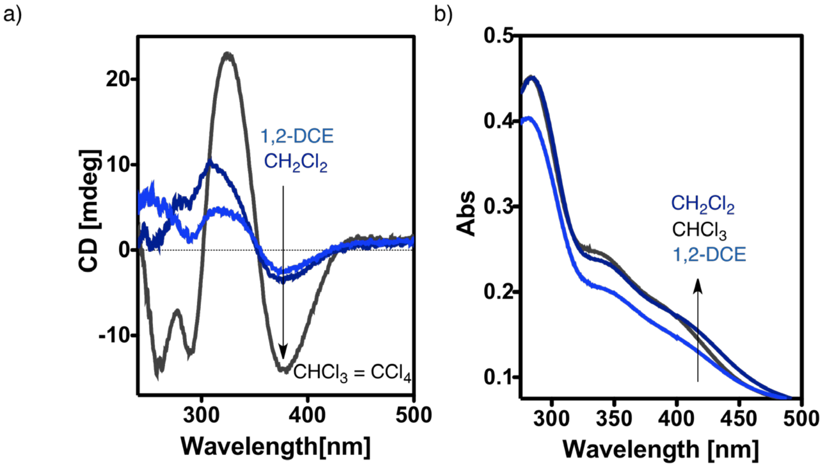

Figure S18: a) CD and b) UV-Vis spectra of poly-(*R*)-**1** in different haloalkanes.

For studying the effect of non-donor and polar solvents such as alcohols, it was necessary to prepare a 0.5 mM solution of poly-(*R*)-**1** using a 3:7 ratio of alcohol/$CHCl_3$ because of solubility issues (see Figure S19).

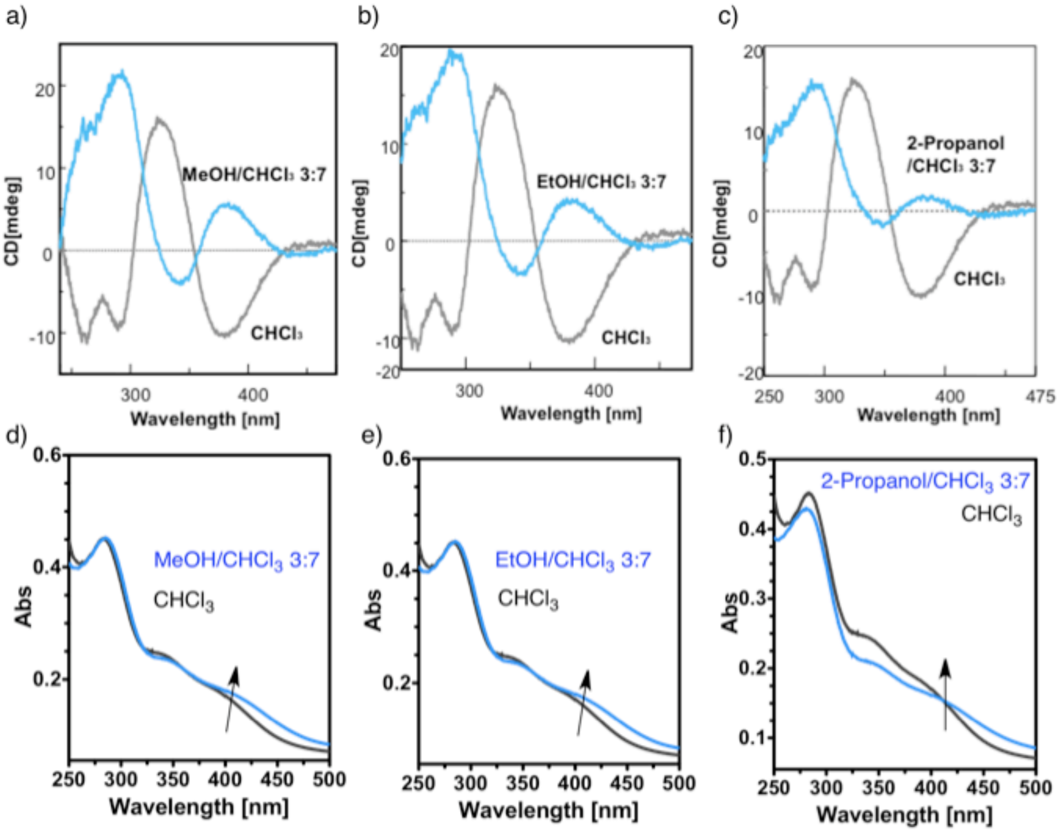

Figure S19: CD and UV-Vis spectra of poly-(*R*)-**1** in different alcohols/$CHCl_3$ mixtures.

CD and UV-Vis studies of poly-(*R*)-1, addition of LiCl

The use of LiCl in combination with solvents such as THF, it is a very well known method to perturb the *cis*-*trans* amide bond equilibria from the major *trans* isomer to the *cis* one. In some of the examples found in literature, it is descrived a difference in the UV-Vis spectrum, where the *cis* isomer has a stronger absorbance in the 275-325 nm region.[IV]

Thus, we prepared a poly-(*R*)-**1** solution in THF and we added up to 2.5 equiv, in order to avoid agregation with the LiCl. The results obtainded reveal an increase of the Cotton effect arround 250-300 nm and at 380 nm. In addition, the UV-Vis reveals an increase of the absorbance arround 280 nm and slight modificantions on the rest of the spectra. The results obtained in two experiments clearly indicate an increase of the *cis* poulation that favors an increase of the helicity too.

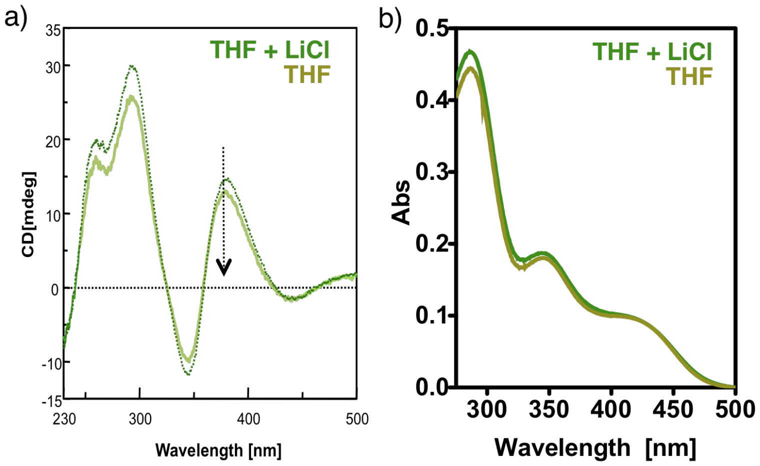

Figure S20: CD a) and UV-Vis b) of poly-(*R*)-**1** in THF and THF + LiCl.

Digest of solvent effects on poly-(*R*)-1 conformation

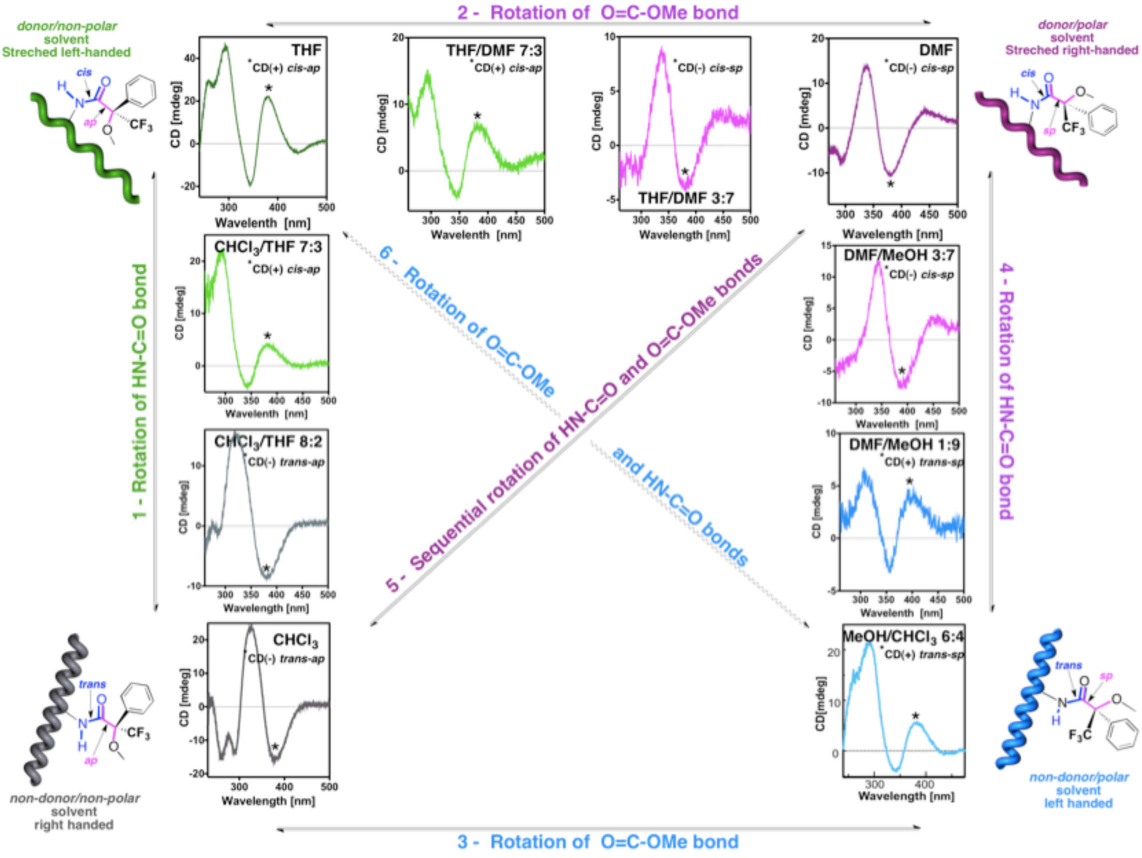

Scheme S4

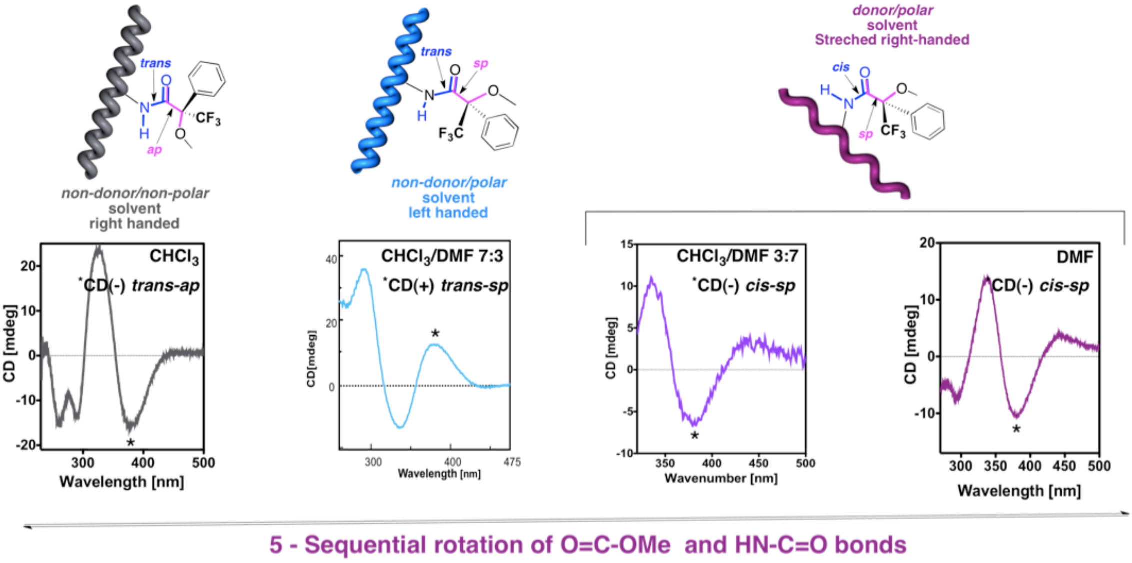

Scheme S5

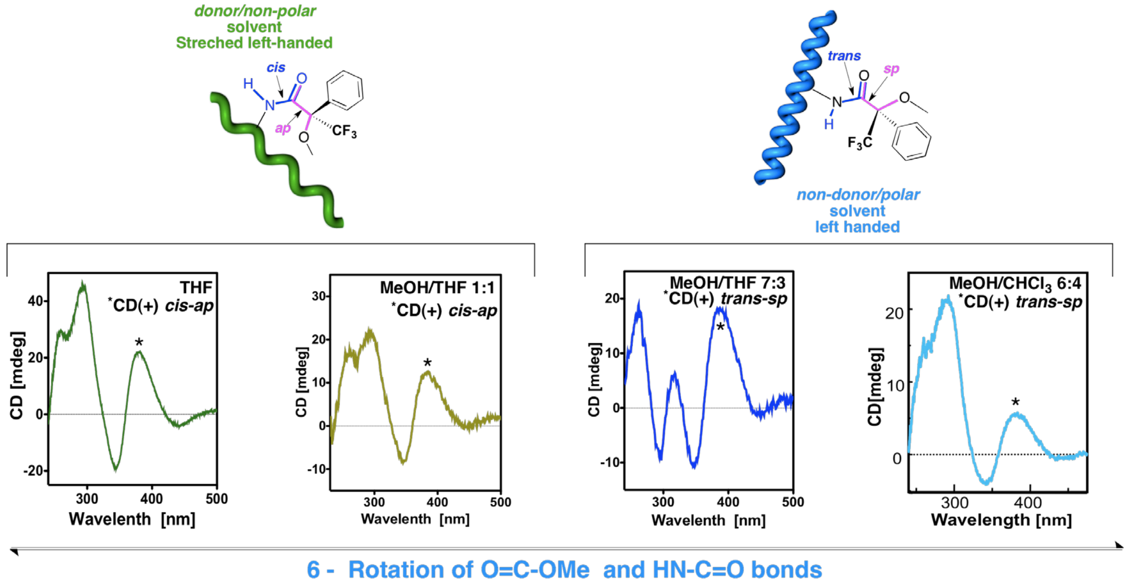
donor/non-polar
solvent
Streched left-handed
cis
H
N
O
ap
O
CF3
trans
sp
O
N
H
O
F3C
non-donor/polar
solvent
left handed
THF
*CD(+) cis-ap
CD [mdeg]
Wavelenth [nm]
MeOH/THF 1:1
*CD(+) cis-ap
CD [mdeg]
Wavelenth [nm]
MeOH/THF 7:3
*CD(+) trans-sp
CD [mdeg]
Wavelenth [nm]
MeOH/CHCl3 6:4
*CD(+) trans-sp
CD[mdeg]
Wavelength [nm]
*
6 - Rotation of O=C-OMe and HN-C=O bonds

Scheme S6

NMR studies in different solvents

^{1}H Spectra in different solvents

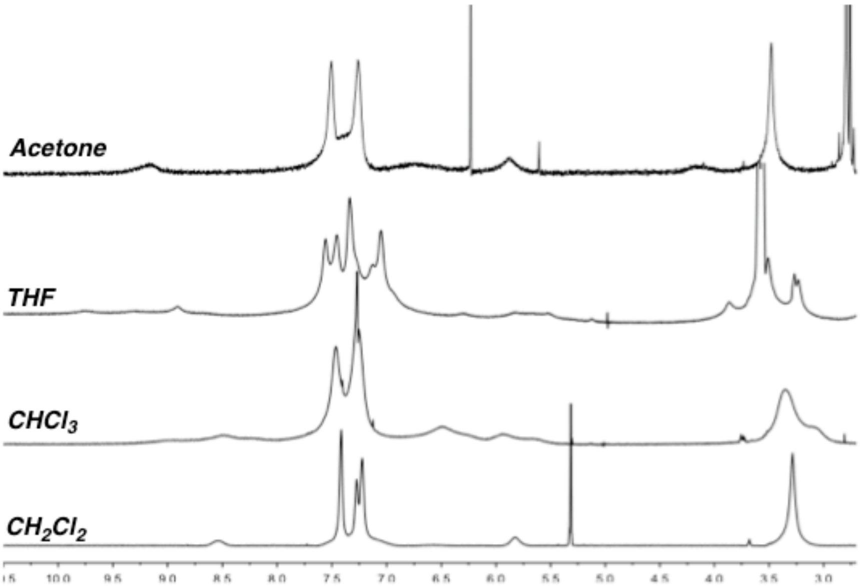

Figure S21: ^{1}H NMR spectra of poly-(*R*)-**1** in different solvents.

^{19}F Spectra in different solvents

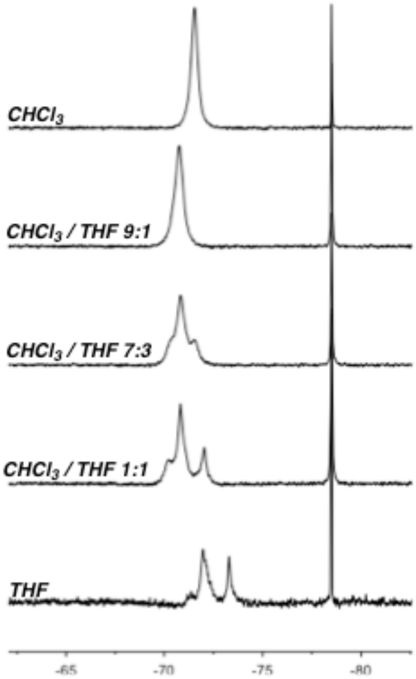

Figure S22: ^{19}F NMR spectra of poly-(*R*)-**1** in different THF-d8/$CDCl_3$ mixtures.

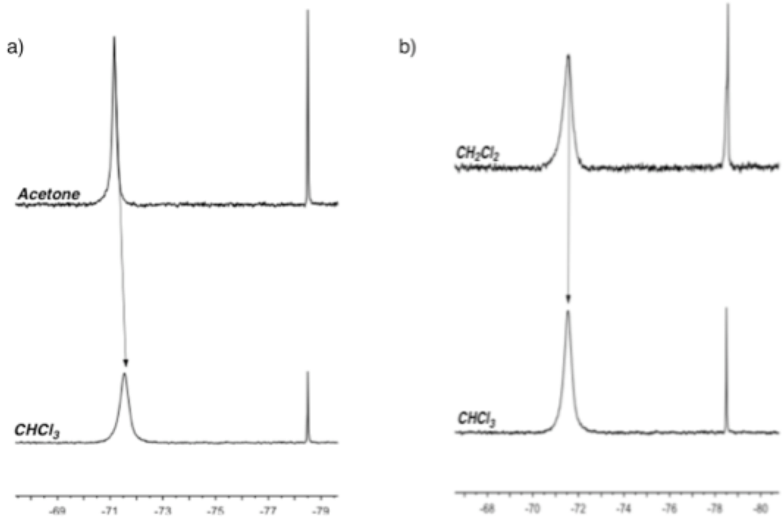

Figure S23: a) ^{19}F NMR spectra of poly-(*R*)-**1** in $CDCl_3$ compared to poly-(*R*)-**1** in acetone-d6 and b) ^{19}F NMR spectra of ^{19}F NMR spectra of poly-(*R*)-**1** in in $CDCl_3$ compared to poly-(*R*)-**1** in CD_2Cl_2.

^{19}F Spectra in different solvents at different temperaturas

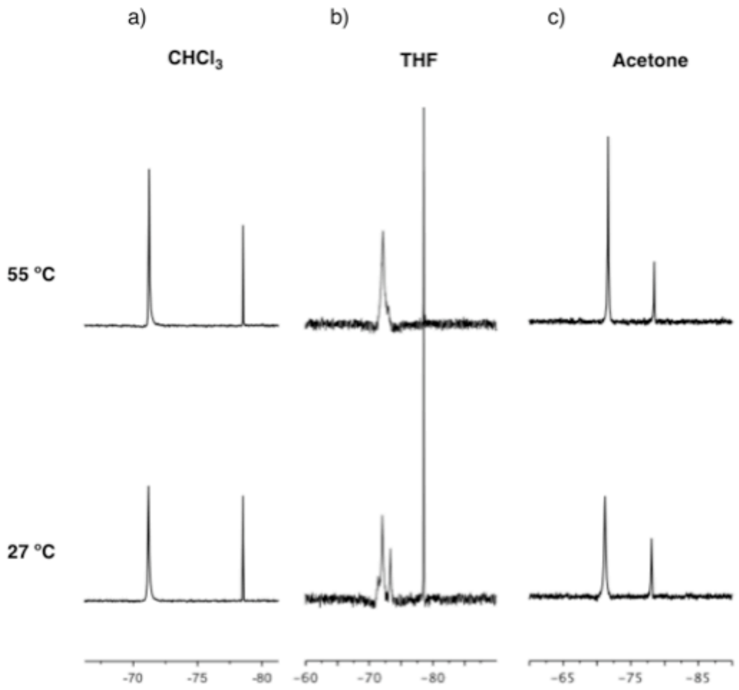

Figure S24: ^{19}F NMR spectra of poly-(*R*)-**1** in a) $CDCl_3$, b) THF-d8 and c) acetone-d6 at different temperatures.

In order to have more precise information about the structural differences of poly-(*R*)-**1** different solvents, NMR experiments were carried out. It is noticeable to see peak displacements and splitting when poly-(*R*)-**1** is dissolved in solvents such as THF-d8 (see Figure S21, Figure S22 and Figure S23). Interestingly, the peak splitting starts at

30% THF-d8 / 70% $CDCl_3$ ratio, which is the minimum amount of THF for inducing helical inversion. In addition, when the poly-(*R*)-**1** solutions are warmed up to 50 ºC, the split peaks merge into a singlet; this fact suggests the presence of aggregation, due to a different conformation of poly-(*R*)-**1** in THF-d8, that is broken when the temperature increases (see Figure S24).

Studies of the effect of donor and non-donor solvents on the conformation of poly-(*R*)-1 by NMR

STD experiments in different solvents

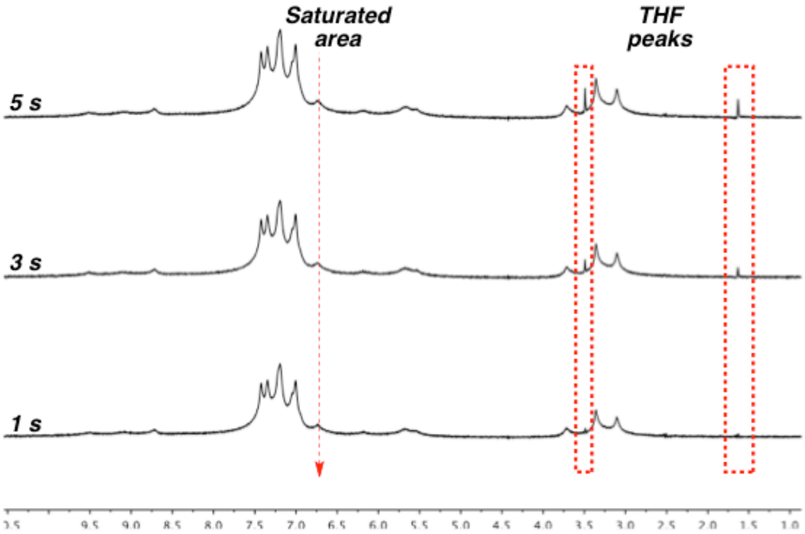

Figure S25: STD experiments of poly-(*R*)-**1** in THF-d8. Saturated peak 6.7 ppm.

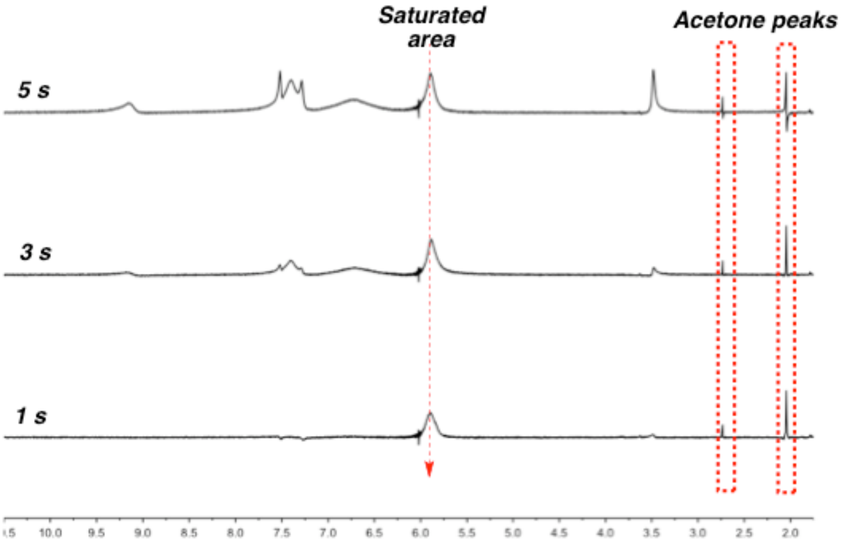

Figure S26: STD experiments of poly-(*R*)-**1** in Acetone-d6. Saturated peak 5.8 ppm.

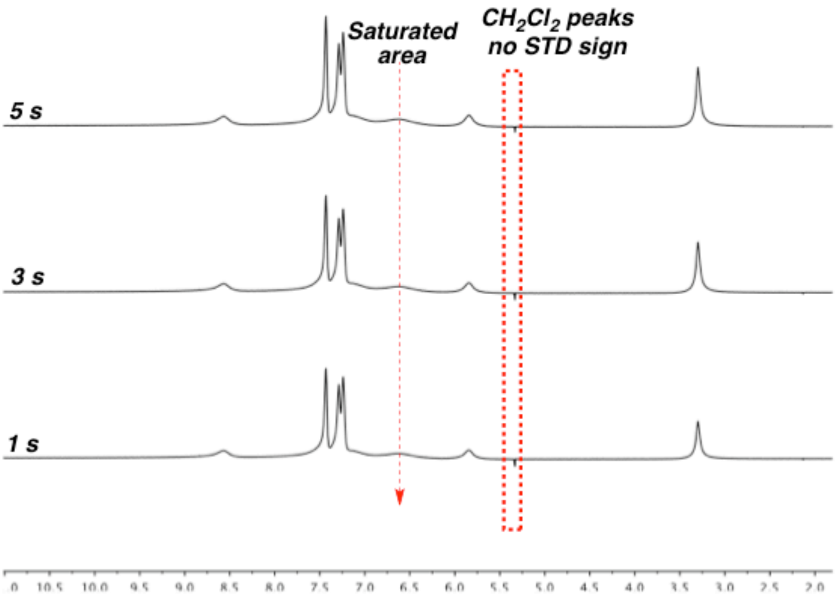

Figure S27: STD experiments of poly-(*R*)-**1** in CD_2Cl_2. Saturated peak 6.7 ppm.

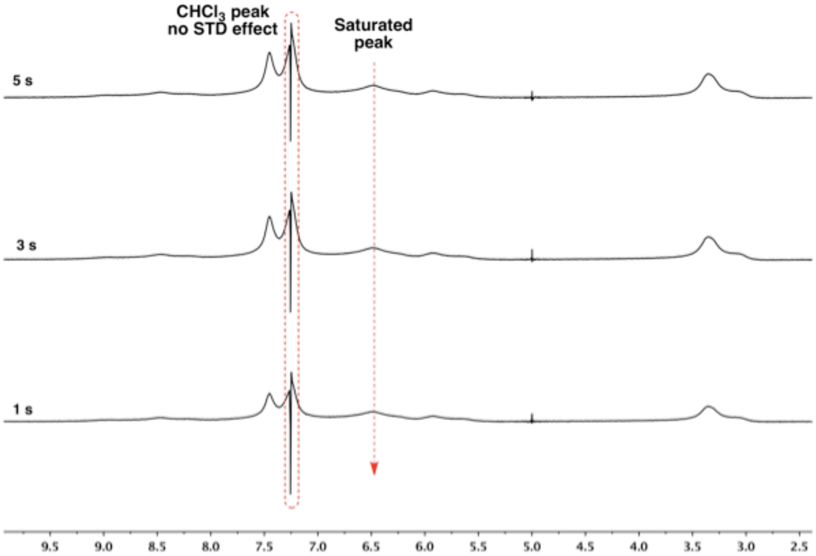

Figure S28: STD-CPMG experiments of poly-(*R*)-**1** in $CDCl_3$. Saturated peak 6.5 ppm.

Saturation transfer difference (STD) experiments were performed in order to study the solvent-polymer interaction. The results show that solvents such as THF-d8 or acetone-d6, donor solvents of different polarities, present STD effects that increase with higher saturation time when the internal protons of the polymer are saturated. Therefore, donor solvents coordinate with poly-(*R*)-**1** (see Figure S25 and Figure S26). On the other hand, when the same experiments were carried out using solvents such as CD_2Cl_2, no STD effect was observed (see Figure S27).

FT-IR Studies

FT-IR spectra were recorded in a BRUKER IFS-66v spectrophotometer. CsI cells were used. A solution of poly-(*R*)-**1** (3 mg/mL) was prepared in THF and $CHCl_3$, respectively. 20µL of these solutions were placed on a CsI cell and the solvent was removed by evaporation. FT-IR experiments show the characteristic NH stretching vibration corresponding to *cis*-phenyl amides in THF.[V]

	poly-(*R*)-**1** in THF	poly-(*R*)-**1** in $CHCl_3$
nNH_{st}	3390 (m) 3325 (m/w)	3389 (m) 3310 (m/w)
CHst	3093 -3033 (w), Ar 2985-2844 (m), OMe	3093 -3033 (w), Ar 2985-2844 (m), OMe
$C{=}O_{st}$ (amide I)	1768 (w) 1701 (s)	- 1705 (s)
$C{=}C_{st}$	1597 (m) 1582 (m)	1595 (m) 1585 (m)
NH_{bend} (amide II)	1517 (s)	1516 (s)
CH (arom)	1450 (w)	1450 (w)
C-HAr/ NHbend	1407 (m)	1404 (m)
CF_3 st	1270 (m)	1271 (m)
OMe st as	1165 (s)	1165 (s)
OMe st sm	1099 (m)	1101 (m)

Table S3: IR stretching vibration of poly-(*R*)-**1** in THF and $CHCl_3$

Optical Rotation Studies

Optical rotation gives useful information about changes on the conformation of the polymer. Measurements for a solution of the poly-(*R*)-**1**, using a concentration of 8 mg/mL, were performed in different solvents. Changes in sign and magnitude indicate that the solvents affect the polymer conformation. (Table S4 and Table S5).

	$CHCl_3$	CH_2Cl_2	THF	Acetone
Poly-(*R*)-**1**	-379.3	+110.0	+655.3	+214.0

Table S4: Optical rotation of poly-(*R*)-**1** in different solvents.

	$CHCl_3$	$CHCl_3$/THF 7:3	$CHCl_3$/THF 1:1	THF
Poly-(*R*)-**1**	-379.3	+384.2	+563.8	+655.3

Table S5: $CHCl_3$/THF titration studies of poly-(*R*)-**1** by optical rotation.

Differencial Scanning Calorimetry (DSC) Studies

DSC experiments were performed for poly-(*R*)-**1** films prepared in THF and $CHCl_3$. The DSC heating traces (300ºC, 10ºC/min) obtained for both films reveal different conformations: *c-t* for THF and *c-c* for $CHCl_3$ (Figure S29).

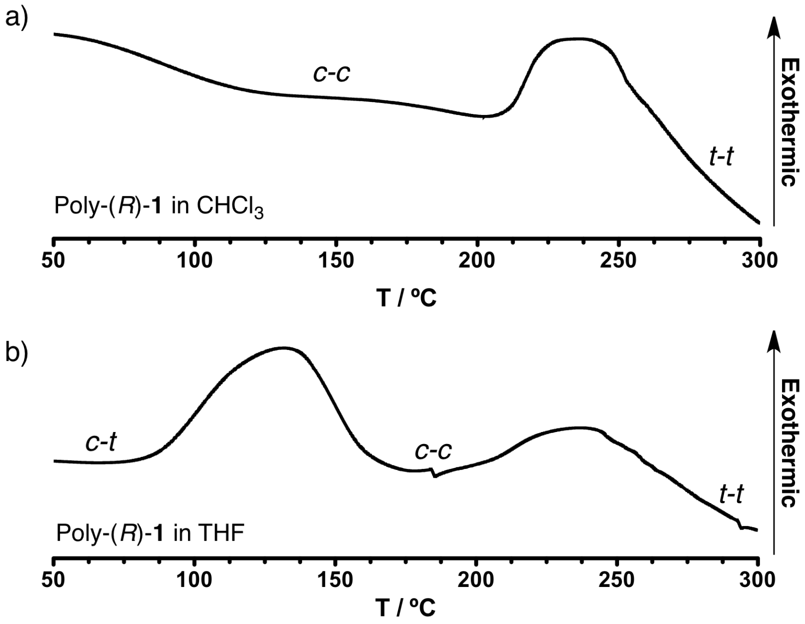

Figure S29: DSC heating traces of poly-(*R*)-**1** films prepared in a) $CHCl_3$ and b) THF.

Both samples were allowed to cool down to 20 ºC at 10ºC/min where no transition peaks were observed (Figure S30).

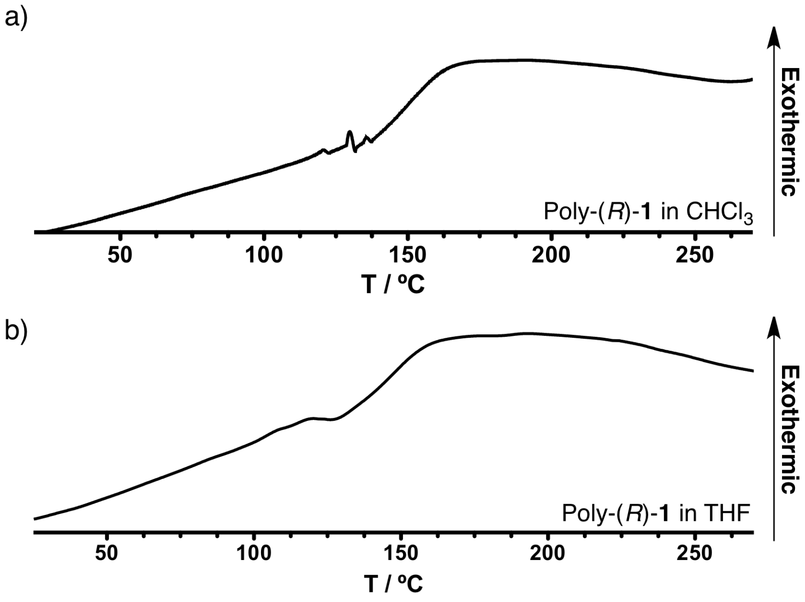

Figure S30: DSC cooling traces of poly-(*R*)-**1** films prepared in a) $CHCl_3$ and b) THF.

Finally, a second heating was done in order to check the reversibility of the process (300ºC, 10ºC/min). Identical DSC traces were obtained for both films, showing the DSC pattern of a *t-t* isomer corresponding to the last transition observed during the first heating in both cases (Figure S31). This fact indicates that the process is not reversible.

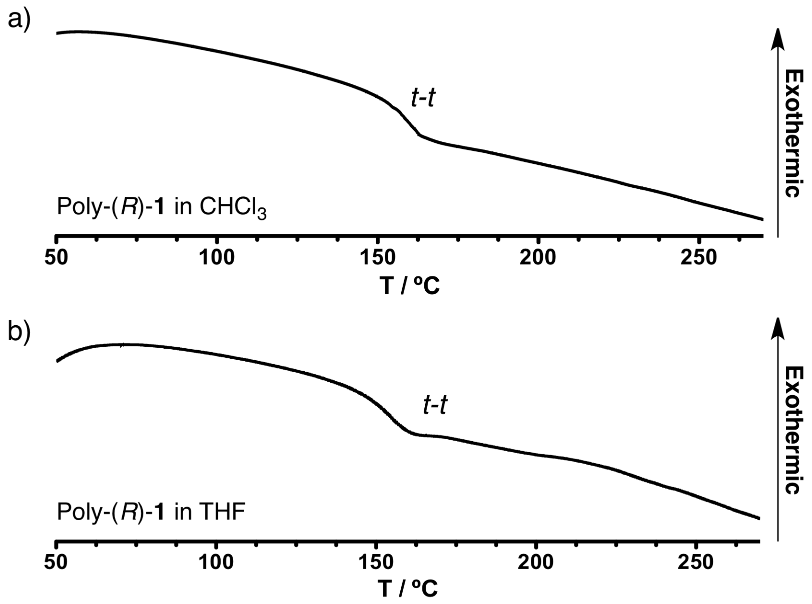

Figure S31: DSC second heating traces of poly-(*R*)-**1** films prepared in a) $CHCl_3$ and b) THF.

Stability of isomers over time and temperature

Poly-(*R*)-**1** film in THF:

In order to study the stability of the *c-t* and *c-c* isomers presented in this paper, DSC studies were carried out. Thus, a poly-(*R*)-**1** film, prepared from a THF solution (*cis-transoidal* configuration, Figure S29b) was heated at 70 ºC for 720 min. The DSC traces show how the *c-t* to *c-c* transition can happen at 70 ºC instead of 132 ºC within 600 min (Figure S32). Next, the poly-(*R*)-**1** sample was allowed to cool down to rt at 10 ºC/min and a second cycle (heating/cooling) was performed. The second heating thermogram (300ºC, 10ºC/min) shows just the *c-c* to *t-t* band (Figure S33), indicating that the *c-t* to *c-c* isomerization is not a reversible process for this polymer. A third heating thermogram over the same sample resulted in a classic DSC trace for a *t-t* conformation, showing also that the *c-c* to *t-t* is not a reversible process (Figure S34).

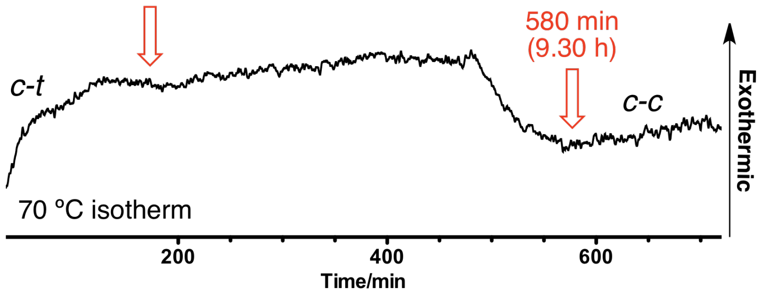

Figure S32: Poly-(*R*)-**1** film prepared in THF, isotherm at 70 ºC.

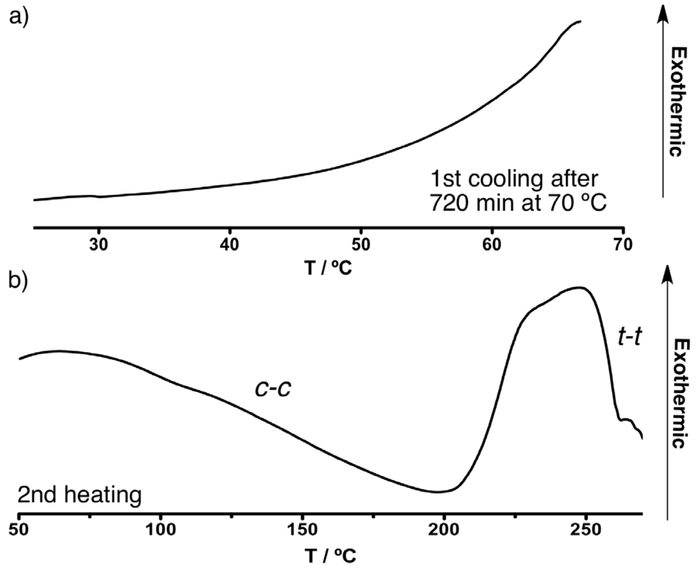

Figure S33: Poly-(*R*)-**1** film prepared in THF, a) 1st cooling and b) 2nd heating processes.

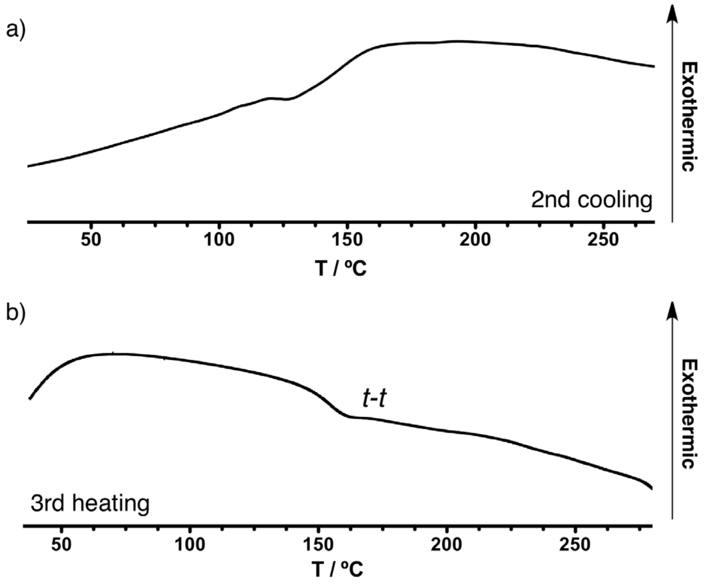

Figure S34: Poly-(*R*)-**1** film prepared in THF, a) 2nd cooling and b) 3rd heating processes.

Poly-(*R*)-**1** film in $CHCl_3$: A similar DSC experiment was performed for a poly-(*R*)-**1** film prepared from a $CHCl_3$ solution (*cis-cisoidal* configuration, Figure S29a). The sample was kept at 200 °C for 800 min. The DSC traces show how the *c-c* to *t-t* transition happens at 200 °C instead of 240 °C during 800 min. After that, the poly-(*R*)-**1** sample was allowed to cool down to 20 °C at 10 °C/min and a second heating/cooling cycle was done. During this second heating process (300 °C at 10 °C/min) a small peak was observed between 225 and 250 °C (Figure S34), corresponding to a residual transition from *c-c* to *t-t* configuration, indicating that the isomerization was not completed during 800 min. A third heating thermogram over the same sample resulted in a classic DSC trace for a *t-t* conformation (Figure S35).

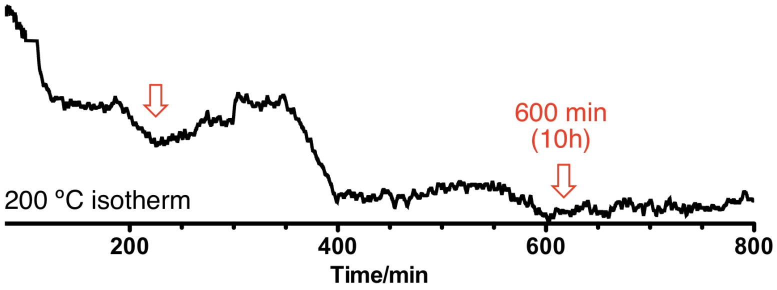

Figure S35: Poly-(*R*)-**1** film, prepared in $CHCl_3$, 200 °C isotherm for 800 min.

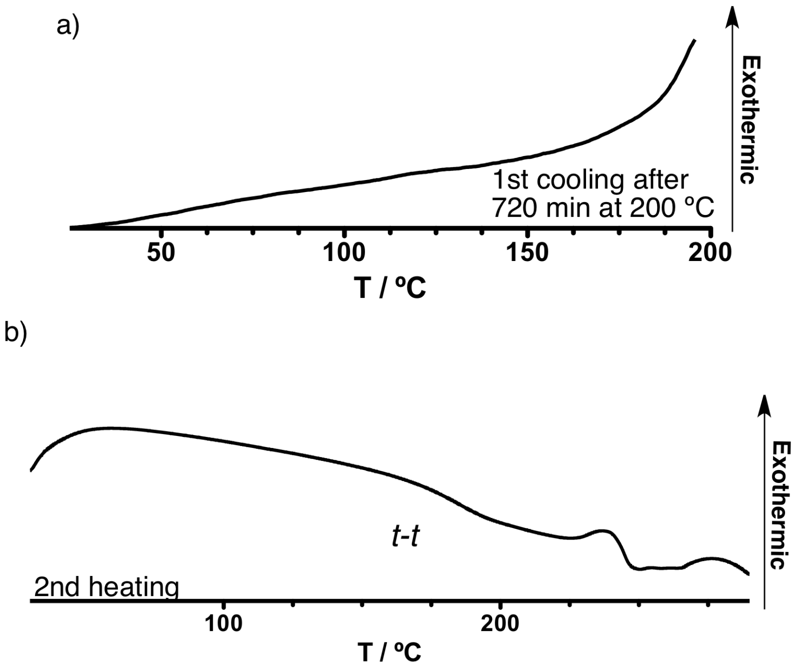

Figure S36: Poly-(*R*)-**1** film prepared in $CHCl_3$, a) 1st cooling and b) 2nd heating processes.

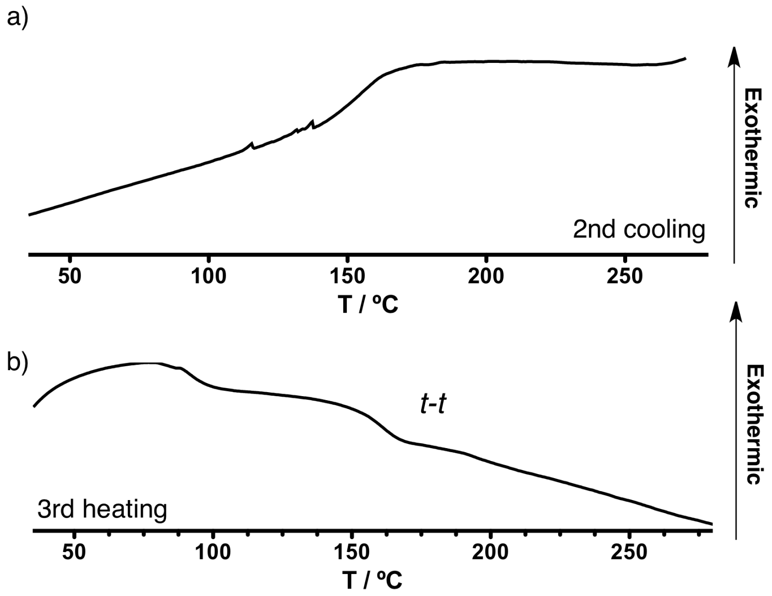

Figure S37: Poly-(*R*)-**1** film prepared in $CHCl_3$, a) 2nd cooling and b) 3rd heating processes.

ESI References

[I] Simionescu, C.I.; Percec, V.; Dumitrescu, S. *J. Polym. Sci., Polym. Chem. Ed.* **1977**, *15*, 2497–2509.

[II] Tabata, M.; Tanaka, Y.; Sadahiro, Y.; Sone, T.; Yokota, K.; Miura, I. *Macromolecules* **1997**, *30*, 5200-5204.

[III] Louzao, I.; Seco, J. M.; Quiñoa, E.; Riguera, R. *Angew. Chem. Int. Ed.* **2010**, *49*, 1430-1433.

[IV] (a) Kofron, J.L.; Kuzmic, P.; Kishore, V.; Colon-Bonilla, E.; Rich, D.H. *Biochemistry*, **1991**, *30*, 6127–6134. (b) Kofron, J. L.; Kuzmic, P.; Kishore, V.; Gemmecker, G.; Fesik, S. W.; Rich, D. H. *J. Am. Chem. Soc.* **1992**, *114*, 2670-2675. (c) Schiene-Fischer, C.; Fischer, G. *J. Am. Chem. Soc.* **2001**, *123*, 6227-6231. (d) Pappenberger, G.; Aygun, H.; Engels, J. W.; Reimer, U.; Fischer, G.; Kiefhaber, T. *Nat. Struct. Biol.* **2001**, *8*, 452-458.

[V] M. Miyazaki, J. Saikawa, H. Ishizuki, T. Taira, M. Fujii; *Phys. Chem. Phys.* **2009**, *11*, 6098-6106.